

# WILD *MUSA* SPP. PSEUDOSTEM AS A NEW SOURCE OF CELLULOSE NANOCRYSTALS

RANJITA NATH and LALDUHSANGA PACHUAU

*Department of Pharmaceutical Science, Assam University, Silchar – 788011, India*

✉ *Corresponding author: L. Pachuau, lalduhsanga.pachuau@aus.ac.in*

*Received March 22, 2022*

The objective of the present work is to investigate the potential of wild *Musa* spp. pseudostem as a sustainable source of cellulose nanocrystals (CNCs). CNCs were isolated from native cellulose by mixed acid hydrolysis under continuous stirring, followed by ultrasonication. CNCs were characterized by various techniques, including SEM, TEM, FTIR and Zeta potential analysis. The thermal stability was investigated through DSC and TGA, while the percent crystallinity was determined by XRD spectroscopy. TEM analysis showed that the isolated CNCs were mostly spherical in shape, with an average diameter of about 102.01 nm. DSC and TGA analyses indicated reduced thermal stability of the CNCs, compared to the native cellulose, which could be explained by the reduced particle size, better thermal conductivity, and active surface functional groups. The findings of the study revealed that the pseudostem of wild *Musa* spp. could be a potential, sustainable source of functional CNCs.

**Keywords:** spherical cellulose nanocrystals, acid hydrolysis, wild banana fibers

## INTRODUCTION

Cellulose nanocrystals derived from botanical sources are an emerging natural and sustainable bionanomaterial bestowed with unique mechanical properties, versatility, amenability to chemical modifications and excellent biodegradability, as well as low cytotoxicity.<sup>1</sup> Several natural plant fibers have been investigated as sources of this nanoscale cellulosic material, but it has been established that the properties of the obtained nanocellulose vary widely depending on the source and hydrolysis conditions.<sup>2</sup> Considering the advantages of such materials, less explored natural bioresources have attracted research interest. In this respect, the pseudostem of wild *Musa* species, commonly available in India, can be an attractive, sustainable candidate for the isolation of cellulose nanocrystals (CNCs). The valorization of such underutilized residues can also be potentially helpful in reducing our dependence on the progressively declining fossil fuels.

One of the interesting attributes of CNCs lies in the possibility to synthesize them in various morphological shapes and sizes. Typically, CNCs are synthesized as rod or needle-shaped crystalline nanoparticles through mineral acid hydrolysis, mainly sulphuric acid at 50-64 wt% under varying conditions.<sup>3-5</sup> However, depending on the treatment before and after the hydrolysis, as well as on the conditions maintained during the hydrolysis of native cellulose, various shapes of CNCs, including spherical, torispherical, ribbon like, needle shape, rectangular, block and network, have also been reported.<sup>6-10</sup> The influence of the morphology on various physicochemical and functional properties of these CNC particles are a subject of interest for future studies.

One of the earliest reports on the synthesis of spherical CNCs used mixed acid (sulphuric acid–hydrochloric acid) hydrolysis of pretreated short-staple cotton cellulose under ultrasonication.<sup>11</sup> The method was later validated on other sources of cellulose, namely, buckeye cellulose<sup>12</sup> and commercial microcrystalline cellulose.<sup>13</sup> Recently, spherical CNCs have also been isolated through acid hydrolysis of cellulose using various concentrations of sulphuric acid, such as 35%,<sup>14</sup> 64% w/v<sup>15</sup> and 65%,<sup>16</sup> by the oxidation method<sup>7,17</sup> and enzymatic hydrolysis.<sup>18,19</sup>

The importance of the non-medicinal part of a drug product, also known as excipient, has been realized over the years by pharmaceutical industries. Traditionally, these inert ingredients are used to facilitate the manufacture, storage, and administration of drug products. However, several studies in recent years have unearthed the roles of these excipients in providing not only manufacturing and application convenience, but also several other high-end functionalities that significantly improve the product's performance *in vivo*.<sup>20-22</sup> It has been shown that these excipients can improve the

bioavailability of the active drug (API) by enhancing its dissolution and membrane permeability, stabilize the product and can also act smart by controlling the release of the API according to the need of the patient.<sup>23</sup> Despite all these developments, however, there is not a single material yet that can perform and satisfy all the functional requirements of such smart drug excipients. Thus, there is an ever-increasing demand for exploring novel functional materials as excipients that would fit the specific performance needs of the drug product to be developed. Cellulose and its derivatives, owing to their safety, functionality, adaptability, and availability, are among the most used excipients in drug delivery and dosage forms.

Therefore, the objective of this work has been to isolate and characterize spherical cellulose nanocrystals (CNCs) from a sustainable and less explored resource – the pseudostem of *Musa* species through mixed acid hydrolysis. Preliminary investigation of the CNCs, focusing on their density and flow properties, was also performed in order to evaluate their functional properties and suitability as tablet excipient in the development of enhanced drug delivery systems.

## EXPERIMENTAL

### Materials

The pseudostems of wild *Musa* spp. was collected from the Aizawl region in Mizoram, India. The plant is locally called *Changthir* in Mizo language, and was identified as *Musa balbisiana*.<sup>24</sup> All the reagents and chemicals used in the experiments were of analytical grade and were used as supplied, without any further purifications.

### Methods

#### *Determination of Klason and soluble lignin content of the fiber*

Klason lignin (acid-insoluble) and acid-soluble lignin were determined following the method described previously.<sup>25</sup> Klason lignin represents the insoluble fractions of 72% H<sub>2</sub>SO<sub>4</sub> treated fibers and soluble lignin was determined by measuring the absorbance of the clear filtrate from the above treatment at 203 nm.

#### *Isolation of cellulose*

*Musa* spp. pseudostems were cut into small pieces of about 1 cm, and were air dried in the laboratory. Cellulose was isolated from the dried pseudostems by following a previously reported procedure,<sup>26</sup> with slight modifications. About 20 g of the dried pseudostems were taken and refluxed with an ethanol/toluene mixture (1:2 v/v ethanol:toluene) for 2 h to dewax and remove other soluble matter, after which it was air dried again. The first step of delignification was performed by heating the sample with 2M NaOH (20 g pseudostem/500 mL 2M NaOH) for 4 h at 80 °C in a water-bath. After 4 h, the solids were filtered off and washed to neutral with water. The alkali treatment and washing to neutrality with water were then repeated once. Repeated bleaching with acidified (acetic acid) 1.3% hydrogen peroxide was performed on the treated biomass as per the reported procedure, after which the product was washed to neutrality with water. The white cellulose product thus obtained was dried in a hot air oven at 50 °C for 72 h and stored in an air-tight container for further processing.

#### *Isolation of cellulose nanocrystals*

Mixed acid hydrolysis was reported by Li *et al.*<sup>11</sup> and was followed in the synthesis of cellulose nanocrystals, with slight modifications. Firstly, the oven-dried cellulose from wild banana pseudostems was treated with dimethyl sulfoxide (DMSO) for 4 h at 80 °C, after which it was thoroughly washed with distilled water and oven-dried again at 50 °C for 72 h. The mixed acid hydrolysis solution was prepared by mixing sulphuric acid, hydrochloric acid and water in the ratio of 3:1:6 (H<sub>2</sub>SO<sub>4</sub>:HCl:Water at 3:1:6). The pretreated cellulose was then hydrolyzed with the mixed acid hydrolyst at 1 g/40 mL (cellulose/hydrolyst) for 6 h at 45 °C, under continuous magnetic stirring at 1000 rpm. After the required time, the milky white colloidal suspension was diluted with two volumes of cold distilled water to stop the hydrolysis. The obtained CNC suspension was dispersed again with a probe ultrasonicator (30 seconds pulsatile) for 30 minutes. The sequence of washing and centrifugation was then performed, followed by oven drying at 50 °C for characterization.

#### *Characterization of cellulose and cellulose nanocrystals (CNCs)*

##### *Moisture content*

Moisture contents of both cellulose and CNCs were expressed in terms of percentage weight loss on drying (% LOD) by drying about 2 g of the samples to a constant weight at 105 °C in an oven for 5 h. The % LOD was then calculated as follows:

$$\% \text{ LOD} = \frac{\text{Weight of water in the sample}}{\text{Total weight of the cellulose/CNC taken}} \times 100 \quad (1)$$

#### *Ash value*

To determine the total ash content, the residual mass remaining at 600 °C in TGA analysis was taken, as previously reported in the literature.<sup>26</sup>

#### *Micromeritics and flow properties*

The true, poured and tapped densities of the samples, along with their porosity, were determined following our previously described method,<sup>27</sup> after the materials were allowed to pass through Sieve No. 10. Powder flow property was also determined by calculating Carr's index and Hausner ratio.

#### *FTIR spectroscopy*

The presence of functional groups was analyzed through Fourier transform infrared spectroscopy (FTIR). The absorbance was recorded for both the cellulose and cellulose nanocrystals isolated from the wild *Musa* spp. pseudostem. The spectra were recorded between 400 and 4000 cm<sup>-1</sup> on an FTIR spectrophotometer (Alpha II FTIR Spectrometer, Bruker).

#### *Hydrodynamic diameter and zeta potential*

To determine the stability of the spherical CNC suspension and its particle size distribution, zeta potential and the hydrodynamic diameter of the cellulose nanocrystals were recorded in a particle size analyzer (Litesizer 500, Anton Paar). Dispersions of the dilute suspension (0.1% w/w) were ultrasonicated for about 15 min before the measurement.

#### *Thermogravimetric analysis*

Thermogravimetric analysis (TGA) was performed to investigate the thermal stability of the samples using a Perkin Elmer TGA 4000, between 35–765 °C, while nitrogen purging was maintained at 20 mL/min. For each analysis, about 5 mg of the sample was taken and the thermograms were recorded for both the isolated cellulose and the prepared cellulose nanocrystals. The residual mass (weight %) remaining at 600 °C was used to estimate the total ash content of the cellulose and the CNCs.<sup>26</sup>

#### *Differential scanning calorimetry*

DSC analysis of the cellulose extracted from wild banana pseudostem and the isolated cellulose nanocrystals was performed on a Perkin Elmer DSC 6000. About 6 mg of the powder sample was taken in an aluminium pan and heated between 35 °C and 765 °C. Nitrogen purging was maintained at 20 mL/min and the empty aluminium pan was used as reference in the analysis.

#### *Electron micrographs*

The shape and surface characteristics of the isolated cellulose was analyzed by scanning electron microscopy (TM 4000 Plus, Hitachi, Japan). Cellulose samples were mounted on the aluminium stub and photomicrographs (SEM) of the fibers were taken after sputter coating with a thin layer of gold.

Transmission electron microscopy (TEM) analysis was also performed for the cellulose nanocrystals after the dried powders were redispersed in an aqueous solvent. TEM micrographs were recorded using a Jeol JEM-2100 PLUS (HR) electron microscope (Japan).

#### *X-ray diffraction analysis*

The X-ray diffraction patterns of both the cellulose and cellulose nanocrystals were recorded on a D8 Advance X-ray Diffractometer (Bruker). The data were collected at 2θ between 5° and 90°. The degree of crystallinity was calculated and expressed as percentage crystallinity index using Segal's method:<sup>28</sup>

$$\text{Crystallinity index (\%)} = \frac{I_{002} - I_{\text{am}}}{I_{002}} \times 100 \quad (2)$$

where  $I_{002}$  is the intensity of the peak at a 2θ angle close to 22°, representing the crystalline portion of the cellulose, and  $I_{\text{am}}$  is the counter reading at peak intensity at 2θ close to 18°, which represents the amorphous portion of the cellulose samples. The percent crystallinity thus calculated was then compared between the cellulose and the cellulose nanocrystals.

#### *Statistical analysis*

The statistical analysis was performed using Microsoft Excel software (Office 365). Data are expressed as means ± SD and the results were taken from independent experiments performed at least in triplicate.

## **RESULTS AND DISCUSSION**

Cellulose was isolated successfully from the pseudostems of wild banana species, *Musa balbisiana*, and then used to extract CNCs by the mixed acid hydrolysis process. The cellulose yield

of the pseudostem (under the experimental conditions used) was found to be 33%, calculated from the dried fiber. The total ash content, as determined from TGA analysis was 4.8% for the cellulose and 1.88% for the CNCs. The reduced ash content in CNC may be the result of solubilization of the ash components and increased purity of CNCs during the strong acid treatments. The Klason lignin content of the crude fiber was determined as  $18.43 \pm 1.22\%$ , while the soluble lignin fraction was found to be 1.51%. The moisture content of the cellulose and the CNCs was determined to be  $6.4 \pm 0.22\%$  and  $6.83 \pm 0.26\%$ , respectively. The % LOD was higher in CNCs, compared to cellulose, which may be due to the higher surface area of the CNCs exposed to the environment, compared to that of native cellulose. The moisture content in cellulose is considered one of the critical attributes that bespeak its quality in pharmaceutical industries.<sup>29</sup> In pharmaceutical tablets, the mechanical properties, such as the tensile strength, compaction and viscoelasticity of cellulose are influenced by the moisture content due the plasticizing effect of water.<sup>30-32</sup> The influence of a moisture content of cellulose above 5% on mechanical properties is more significant, and pharmacopoeias permit moisture contents up to 6-7% for cellulose products such as microcrystalline cellulose (MCC) for pharmaceutical industries.<sup>27</sup> Both the cellulose and the isolated CNCs are found to be within the permitted moisture content for cellulose products, as provided in pharmacopoeias.

The science and technology of small particles is referred to as micromeritics. Several micromeritic properties are indicators of the material's suitability as a functional excipient in pharmaceutical preparations. The results of the micromeritic studies are given in Table 1. The powder flow property can be evaluated by determining the values of Carr's index (CI) and Hausner ratio (HR) for the powder. CI indicates the strength of the powder bridge and stability, while HR measures the interparticulate friction.<sup>33</sup> The CI and HR values obtained for the isolated CNCs indicate passable flow and a porous material, but the values are close to those previously reported for spray-dried CNFs.<sup>34</sup>

### **FTIR spectroscopy**

Figure 1 illustrates the FTIR spectra of the cellulose and the CNCs. On observing the spectra, the samples exhibit similarity in their characteristic IR absorption spectra, indicating that the basic structure or the characteristic cellulose fingerprint remains intact, even after the harsh alkali and strong acid treatments. A broad band with peaks at  $3327.64 \text{ cm}^{-1}$ , occurring in both the cellulose and CNCs, can be attributed to the stretching vibrations of the -O-H group present in cellulose, resulting from the presence of moisture in the samples. Banana pseudostems are lignocellulosic in nature, with the presence of different oxygen-containing functional groups, including OH, C=O, C-O-C and C-O-H.<sup>35,36</sup> The peaks at  $2891$  and  $2888 \text{ cm}^{-1}$  in the cellulose and CNCs, respectively, are due to the CH stretching peaks attributed to the crystalline order of cellulose.<sup>27</sup>

Table 1  
Summary of physicochemical properties of wild banana cellulose and CNCs

Sr. No.	Property	Cellulose	CNCs
1	Moisture content	$6.4 \pm 0.22 \%$	$6.83 \pm 0.26$
2	Ash value	4.8%	1.88%
3	True density (g/mL)	-	1.489
4	Carr's index	-	22.91
5	Hausner ratio	-	1.297
6	Porosity	-	0.847
7	Crystallinity index	66.40%	72.08%
8	Average size of spherical CNCs	-	$102.01 \pm 78.17 \text{ nm}$
9	T <sub>50</sub> °C in TGA	347.82 °C	338.81 °C
10	T <sub>max</sub> in DSC	348.42 °C	343.85 °C
11	Zeta potential	-	-6.3 mV

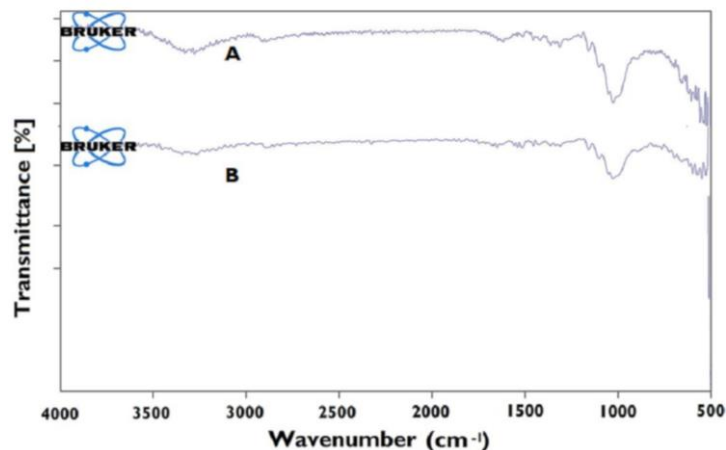


Figure 1: FTIR spectra for (A) cellulose and (B) CNCs

An absorption peak around  $1740\text{--}1730\text{ cm}^{-1}$  is assigned to the acetyl or uronic ester groups of the hemicelluloses or to the ester linkage of carboxylic group present in lignin or hemicelluloses.<sup>35,37</sup> These peaks were not detected in the samples. However, miniscule peaks were detected at  $1515$  and  $1514\text{ cm}^{-1}$ , respectively, in the cellulose and CNC samples, which could be attributed to the aromatic stretching vibrations of  $\text{-C=C-}$  in lignins.<sup>35,36</sup> These peaks indicate the presence of aromatic residues in both samples, however, the peaks become even less prominent in the CNCs, compared to the cellulose sample. The peaks observed at  $1418$  and  $1422\text{ cm}^{-1}$ , respectively, in cellulose and CNCs are also called ‘the crystallinity band’, due to the symmetric  $\text{-CH}_2\text{-}$  bending vibration.<sup>27</sup> The  $\text{-C-H}$  asymmetric deformation peaks for cellulose and CNCs were detected at  $1316$  and  $1313\text{ cm}^{-1}$ , respectively. The C-O-C pyranose ring skeletal vibration peak was traced at  $1026$  and  $1028\text{ cm}^{-1}$ , respectively, in cellulose and CNCs.<sup>35,37</sup> The peaks attributed to the  $\beta$ -glycosidic linkage vibration in the cellulose were observed between  $800\text{--}900\text{ cm}^{-1}$  in both samples.

### Morphology

The morphology of the isolated cellulose and the CNCs was examined through SEM and TEM studies, and the micrographs are shown in Figure 2. SEM results showed that the native cellulose is composed of long and thin microfibrils, forming a network structure, and their average width is about  $10\text{ }\mu\text{m}$ .

The source of extraction, hydrolysis time and the method of production have been found to be important parameters in determining the size and morphology of the isolated nanocellulose. Recently, nanocellulose was isolated from the pseudostem of *M. acuminata x balbisiana* through 1 to 2 hours HCl hydrolysis of  $\alpha$ -cellulose obtained from the pseudostem, followed by ultrasonication.<sup>38</sup> The nanocellulose isolation process was reported to yield fibers with  $69\text{ nm}$  width and several  $\mu\text{m}$  in length. Ultrasonication of  $60\text{ wt}\%$   $\text{H}_2\text{SO}_4$  (45 minutes) hydrolyzed nanocellulose from date palm leaflets was also reported to yield a much reduced size of  $\leq 50\text{ nm}$ .<sup>39</sup> However, the specific diameter or length of the cellulose nanocrystals were not reported. The influence of hydrolysis time and post-hydrolysis treatment on the morphology of cellulose nanocrystals was also reported by de Oliveira *et al.*<sup>40</sup> Enzymatic hydrolysis of rice husks, oat husks and eucalyptus fibers for 5 days, followed by high pressure homogenization, produced cellulose nanocrystals of spherical or close to spherical morphology, with the diameter ranging from  $16.0$  to  $28.8\text{ nm}$ . Also,  $\text{H}_2\text{SO}_4$  hydrolysis of biomass from *Enteromorpha prolifera* for 50 min, followed by 10 min ultrasonication, was reported by Kazharska *et al.*<sup>41</sup> to yield cellulose nanocrystals with needle-shaped morphology, having a length of  $177\pm 12\text{ nm}$  and a width of  $3\pm 1\text{ nm}$ .

The observation of TEM micrographs in the present study has revealed that nanoscale cellulose crystals can be isolated from the wild banana fiber under investigation through mixed acid hydrolysis. Most of the CNC particles observed under TEM exhibit spherical or close to spherical morphology, however, the presence of a few low aspect ratio rod-shaped CNC particles was also noticed. In addition, the aggregation of the particles was observed in all the slides, which may be attributed to the drying process during which strong intermolecular hydrogen bond formations may occur among the

CNC particles.<sup>7</sup> Using an ImageJ software, the size distribution of the CNC particles was measured. The average size of the spherical CNC particles was found to be  $102.01 \pm 78.17$  nm. The average width of the rod-shaped particle fractions was 32.49 nm and the average length was 162.14 nm with an aspect ratio calculated at around 5.

Thus, the procedure employed in the present study involving mixed acid hydrolysis and post-hydrolysis ultrasonication was found to yield cellulose nanocrystals, with different morphology from that of similar nano-materials recently reported in the literature. The isolated cellulose nanocrystals, due to their size and spherical morphology, have the potential to be used in the development of co-processed excipient for pharmaceutical tablet manufacturing. Thus, further investigations will be conducted to develop a starch-based co-processed excipient and its rapid disintegration properties will be evaluated in future work.

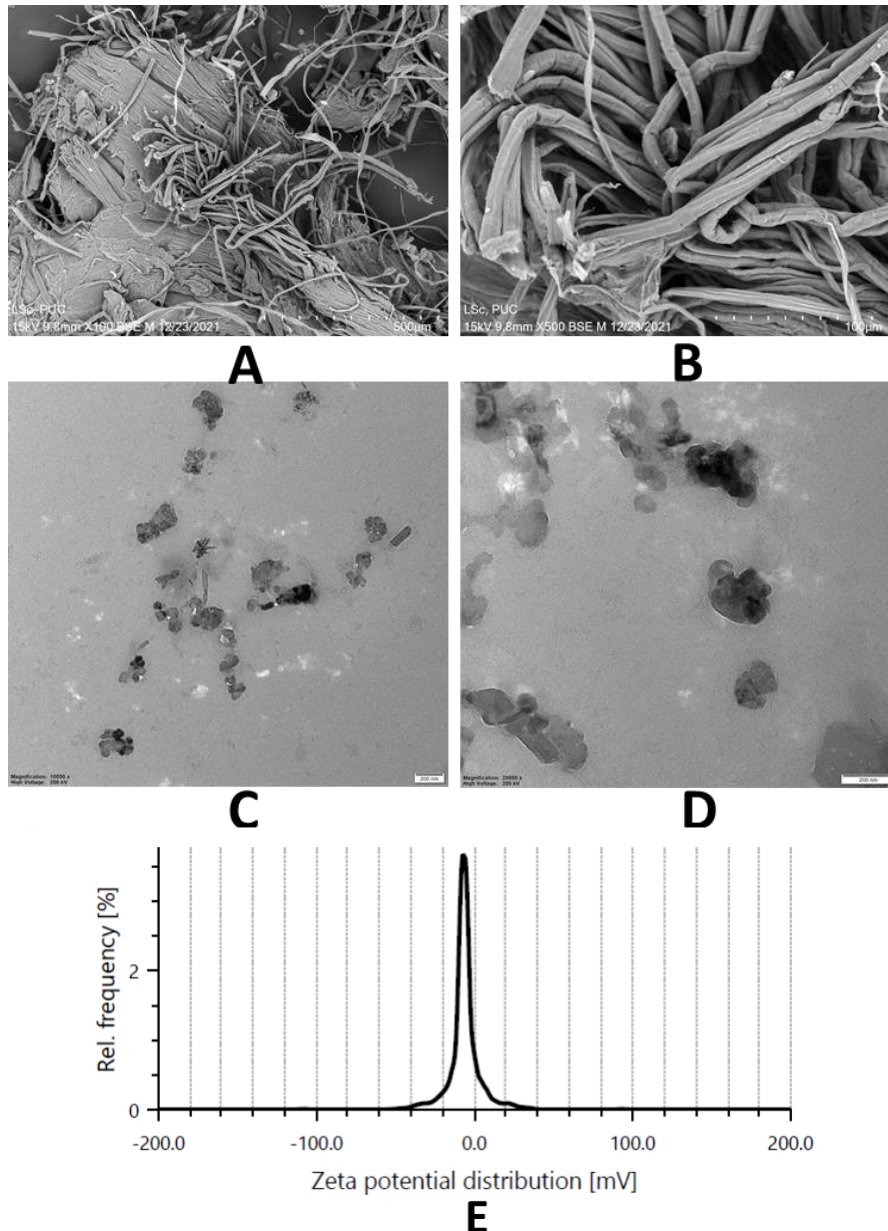


Figure 2: SEM micrographs of cellulose (A: scale bar = 500 μm, B: scale bar = 100 μm); TEM micrographs of CNCs (C and D: scale bar = 200 nm), Zeta potential (E)

### Zeta potential and hydrodynamic diameter

Zeta potential (Fig. 2E) is an important indicator of the system's thermodynamic stability. The measurement of the zeta potential of the CNCs shows that a value of -6.3 mV, indicating the comparatively low stability of the system, which may result from the dilution and washing of the CNCs during the processing for zeta measurement. The low stability of the system was also confirmed by the aggregation of particles taking place during storage as the hydrodynamic diameter of the particles increased to 178.66  $\mu\text{m}$  due to the aggregation of the nanometer-sized particles.

### Thermal property

The thermal properties and stability of the CNCs was investigated through TGA and DSC analyses and compared to those of the wild banana cellulose from which they were isolated; the thermograms are shown in Figure 3. As observed from the thermograms, the thermal degradation of the isolated CNCs and cellulose is a multistep event. The CNCs were also found to exhibit different degradation behavior, as compared to that of the original cellulose from which it was isolated. The first thermal event for both the CNCs and cellulose started at about 60  $^{\circ}\text{C}$ , which can be attributed to the loss of loosely bound water and most of the bound or chemisorbed water is evaporated at about 120  $^{\circ}\text{C}$ .<sup>5</sup> At 120  $^{\circ}\text{C}$ , there was 7.02% total weight loss in the CNCs, and the corresponding weight loss in the source cellulose was 6.72%. Generally, acid hydrolyzed CNCs,<sup>6,42</sup> as well as CNCs obtained by oxidation,<sup>17</sup> are known to exhibit lower thermal stability than their original cellulose fibers. There are three important factors that led to the lower thermal stability of CNCs, compared to their cellulose sources.<sup>5,6,17</sup> Firstly, the smaller particle size resulted in the exposure of a larger surface area to the supplied heat, leading to reduced thermal stability in the CNCs. Secondly, there is a faster heat transfer in the CNCs facilitated by the small phonon scattering of the crystalline chains of the CNCs, as compared to the random chains of the cellulose, leading to better thermal conductivity. Thirdly, the introduction of sulfate groups by the sulphuric acid hydrolysis lowered the activation energy of degradation.

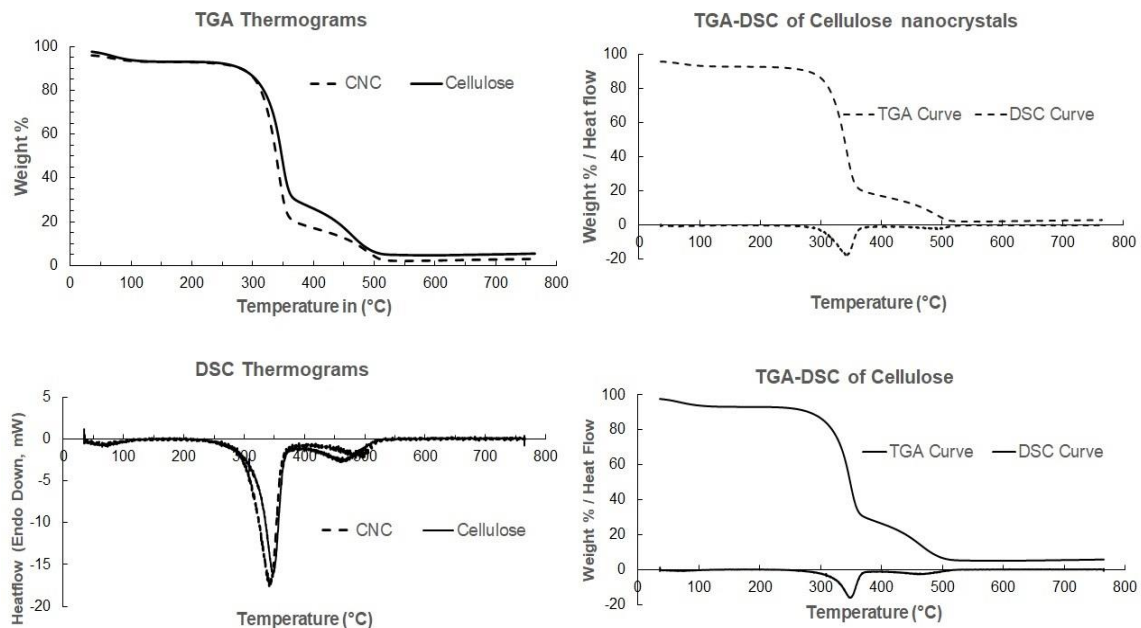


Figure 3: TGA and DSC thermograms of cellulose and CNCs

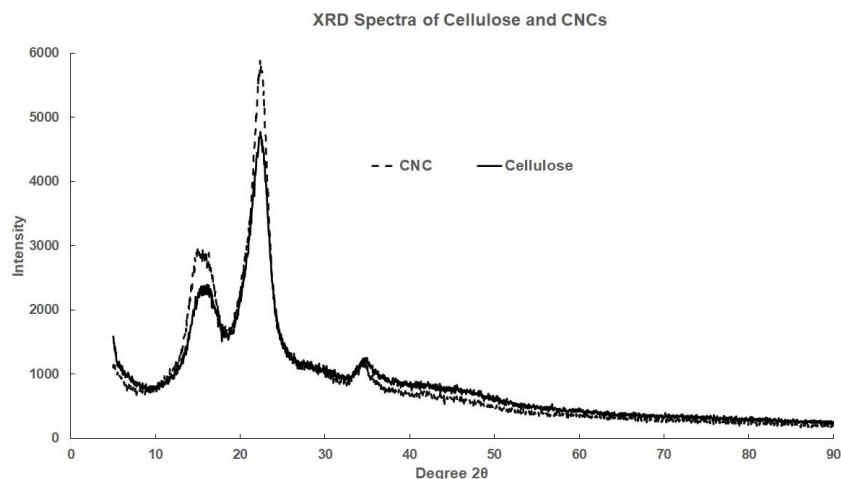


Figure 4: XRD diffractograms of cellulose and CNCs

Following a gradual, negligible weight loss up to about 240 °C, the second major thermal degradation event in both the isolated CNCs and the cellulose occurred at 300–365 °C, where there is a sharp weight loss attributed to pyrolysis of crystals involving various decomposition–gasification processes.<sup>6</sup> This sharp weight loss is much more remarkable in the CNC sample than in the source cellulose, as there is about 68.79% weight loss in CNCs during this event and about 55.71% weight loss in the source cellulose. As evident from the DSC curve, the maximum degradation temperature ( $T_{\max}$ ) for CNCs occurred at 343.85 °C and at 348.42 °C for the cellulose. The temperature at which 50% weight loss occurred ( $T_{50}$  °C) is 338.81 °C and 347.82 °C for the CNCs and the cellulose, respectively. The sharp thermal weight loss is followed by a more gradual, less steep weight loss in both samples. The residual weight (wt%) at 600 °C, which is also used to calculate the ash value in this work, is 1.88% for the CNCs and 4.8% for the source cellulose. The results from the TGA and DSC analyses revealed that the isolated CNCs from wild banana pseudostem exhibit lower thermal stability, as compared to the source cellulose, owing to its smaller size, better thermal conductivity and active surface groups introduced during the hydrolysis procedure. Similar findings have also been reported previously on CNCs isolated from sugarcane bagasse,<sup>43</sup> as well as from rice, oat and eucalyptus.<sup>40</sup>

#### ***X-ray diffraction and percent crystallinity***

Powder XRD spectroscopy is used to investigate the crystallinity of materials and study the relationship between the crystal structure of a solid substance and its physical, mechanical, and chemical properties.<sup>44</sup> In pharmaceutical preparations, the crystallinity of API and excipients plays an important role during tablet compression, and can determine their stability, dissolution, and bioavailability.<sup>45</sup>

In the present study, XRD spectroscopy was carried out to determine the crystallinity index for both the isolated cellulose and the CNCs. The X-ray diffraction (XRD) patterns of the source cellulose and the CNCs are depicted in Figure 4. The structure of cellulose is not entirely crystalline, as it also contains disordered, amorphous domains within its structure. Acid treatments easily removed this disordered, amorphous region, while the more ordered crystalline region remained intact, due to its resistance to acid hydrolysis.<sup>46</sup> The crystallinity index can be used to describe the relative amount of the crystalline and amorphous domains in the cellulose samples. Segal's method<sup>28</sup> was used in the calculation of the crystallinity index in the current study. The crystallinity index calculated for the native cellulose was 66.4% and 72.08% for the CNCs. As expected, acid hydrolysis of the native cellulose isolated from the wild banana fiber degraded the amorphous regions of the cellulose, resulting in higher percent crystallinity of the CNCs. The increase in the crystallinity of cellulose nanocrystals, compared to that of native cellulose, was also reported for cellulose nanocrystals from date palm tree.<sup>39</sup> The relative crystallinity of cellulose nanocrystals from rice, oat, and eucalyptus was reported to be 60.0%, 90.0%, and 95.1%, respectively.<sup>40</sup>

## CONCLUSION

Cellulose is considered to be one of the most sustainable and functional materials of the 21<sup>st</sup> century. Due to its amenability to various surface modifications and tunability to suit the specific needs of the application area, cellulose has become one of the most important materials to substitute synthetic plastics in various industries. Judicious utilization of bioresources has thus become a sensible approach to meet our need of sustainable and renewable alternatives to petroleum-based products with lower carbon footprints. The present study demonstrates the potential of a less known bioresource – wild *Musa* spp. pseudostem – as a source of functional CNCs for biomedical applications, especially towards the development of enhanced drug delivery systems. Preliminary investigations on the physicochemical properties of the obtained CNCs and their solid-state characterization demonstrate their potential for such applications.

**ACKNOWLEDGEMENT:** The authors are grateful to SERB, Department of Science and Technology, Government of India, for the research grant to Dr. Laldhusanga Pachau (Project No. EEQ/2019/000112) and the Junior Research Fellowship to Ms. Ranjita Nath at Assam University, Silchar, India. They also acknowledge and are grateful to the Institute of Advanced Study in Science and Technology (IASST), Guwahati, for TEM, XRD, DSC and TGA studies. Prof. Bhaskar Mazumder and Mr. Rajat S. Dutta are thanked for FTIR analysis and Zeta size measurements, and the Department of Life Sciences, Pachhunga University College, for SEM studies.

## REFERENCES

- <sup>1</sup> R. M. Domingues, M. E. Gomes and R. L. Reis, *Biomacromolecules*, **15**, 2327 (2014), <https://doi.org/10.1021/bm500524s>
- <sup>2</sup> Y. Habibi, L. A. Lucia and O. J. Rojas, *Chem. Rev.*, **110**, 3470 (2010), <https://doi.org/10.1021/cr900339w>
- <sup>3</sup> H. Doh, M. H. Lee and W. S. Whiteside, *Food Hydrocoll.*, **102**, 105542 (2020), <https://doi.org/10.1016/j.foodhyd.2019.105542>
- <sup>4</sup> K. S. Prado and M. A. S. Spinace, *Int. J. Biol. Macromol.*, **122**, 410 (2019), <https://doi.org/10.1016/j.ijbiomac.2018.10.187>
- <sup>5</sup> C. Verma, M. Chhajer, P. Gupta, S. Roy and P. K. Maji, *Int. J. Biol. Macromol.*, **175**, 242 (2021), <https://doi.org/10.1016/j.ijbiomac.2021.02.038>
- <sup>6</sup> P. Lu and Y. Hsieh, *Carbohydr. Polym.*, **82**, 329 (2010), <https://doi.org/10.1016/j.carbpol.2010.04.073>
- <sup>7</sup> D. Yang, X. Peng, L. Zhong, X. Cao, W. Chen *et al.*, *Cellulose*, **20**, 2427 (2013), <https://doi.org/10.1007/s10570-013-9997-0>
- <sup>8</sup> D. Zheng, Y. Deng, Y. Xia, Y. Nan, M. Peng *et al.*, *BioResources*, **14**, 7763 (2019), <https://doi.org/10.15376/biores.14.4.7763-7774>
- <sup>9</sup> D. Zheng, Y. Zhang, Y. Guo and J. Yue, *Polymers*, **11**, 1130 (2019), <https://doi.org/10.3390/polym11071130>
- <sup>10</sup> Y. Zhou, T. Saito, L. Bergstrom and A. Isogai, *Biomacromolecules*, **19**, 633 (2018), <https://doi.org/10.1021/acs.biomac.7b01730>
- <sup>11</sup> X. Li, E. Ding and G. Li, *Chin. J. Polym. Sci.*, **19**, 291 (2001)
- <sup>12</sup> J. Zhang, T. J. Elder, Y. Pu and A. J. Ragauskas, *Carbohydr. Polym.*, **69**, 607 (2007), <https://doi.org/10.1016/j.carbpol.2007.01.019>
- <sup>13</sup> N. Wang, E. Ding and R. Cheng, *Langmuir*, **24**, 5 (2008), <https://doi.org/10.1021/la702923w>
- <sup>14</sup> B. S. Purkait, D. Ray, S. Sengupta, T. Kar, A. Mohanty *et al.*, *Ind. Eng. Chem. Res.*, **50**, 871 (2011), <https://doi.org/10.1021/ie101797d>
- <sup>15</sup> Z. A. Zianor Azrina, M. D. H. Beg, M. Y. Rosli, R. Ramli, N. Junadi *et al.*, *Carbohydr. Polym.*, **162**, 115 (2017), <https://doi.org/10.1016/j.carbpol.2017.01.035>
- <sup>16</sup> C. Trilokesh and K. B. Uppuluri, *Sci. Rep.*, **9**, 16709 (2019), <https://doi.org/10.1038/s41598-019-53412-x>
- <sup>17</sup> M. Cheng, Z. Qin, Y. Liu, Y. Qin, T. Li *et al.*, *J. Mater. Chem. A*, **2**, 251 (2014), <https://doi.org/10.1039/C3TA13653A>
- <sup>18</sup> N. Satyamurthy and N. Vigneshwaran, *Enzyme Microb. Technol.*, **52**, 20 (2013), <https://doi.org/10.1016/j.enzmictec.2012.09.002>
- <sup>19</sup> J. Xu, X. Chen, W. Shen and Z. Li, *Carbohydr. Polym.*, **256**, 117493 (2021), <https://doi.org/10.1016/j.carbpol.2020.117493>
- <sup>20</sup> V. S. Dave, S. D. Saoji, N. A. Raut and R. V. Haware, *J. Pharm. Sci.*, **104**, 906 (2015), <https://doi.org/10.1002/jps.24299>
- <sup>21</sup> J. Hamman and J. Steenekamp, *Expert Opin. Drug Deliv.*, **9**, 219 (2012), <https://doi.org/10.1517/17425247.2012.647907>
- <sup>22</sup> H. Kalasz and I. Antal, *Curr. Med. Chem.*, **13**, 2535 (2006), <https://doi.org/10.2174/092986706778201648>

- <sup>23</sup> M. Hruby, S. K. Filippov and P. Stepanek, *Eur. Polym. J.*, **65**, 82 (2015), <https://doi.org/10.1016/j.eurpolymj.2015.01.016>
- <sup>24</sup> L. Pachuau, A. D. Atom and R. Thangjam, *Appl. Biochem. Biotechnol.*, **172**, 3939 (2014), <https://doi.org/10.1007/s12010-014-0827-0>
- <sup>25</sup> C. W. Dence, in “Methods in Lignin Chemistry”, edited by S. Y. Lin and C. W. Dence, Springer-Verlag, 1992, pp. 33-61
- <sup>26</sup> S. Mueller, C. Weder and E. J. Foster, *RSC Adv.*, **4**, 907 (2014), <https://doi.org/10.1039/C3RA46390G>
- <sup>27</sup> L. Pachuau, R. S. Dutta, L. Hauzel, T. B. Devi and D. Deka, *Carbohydr. Polym.*, **206**, 336 (2019), <https://doi.org/10.1016/j.carbpol.2018.11.013>
- <sup>28</sup> L. Segal, J. J. Creely, A. E. Martin and C. M. Conrad, *Text. Res. J.*, **29**, 786 (1959), <https://doi.org/10.1177/004051755902901003>
- <sup>29</sup> G. Thoorens, F. Krier, B. Leclercq, B. Carlin and B. Evrard, *Int. J. Pharm.*, **473**, 64 (2014), <https://doi.org/10.1016/j.ijpharm.2014.06.055>
- <sup>30</sup> G. E. Amidon and M. E. Houghton, *Pharm. Res.*, **12**, 923 (1995), <https://doi.org/10.1023/A:1016233725612>
- <sup>31</sup> K. A. Khan, P. Musikabhumma and J. P. Warr, *Drug Develop. Ind. Pharm.*, **7**, 525 (1981), <https://doi.org/10.3109/03639048109057729>
- <sup>32</sup> C. C. Sun, *Int. J. Pharm.*, **346**, 93 (2008), <https://doi.org/10.1016/j.ijpharm.2007.06.017>
- <sup>33</sup> R. B. Shah, M. A. Tawakkul and M. A. Khan, *AAPS PharmSciTech*, **9**, 250 (2008), <https://doi.org/10.1208/s12249-008-9046-8>
- <sup>34</sup> R. Kolakovic, L. Peltonen, T. Laaksonen, K. Putkisto, A. Laukkanen *et al.*, *AAPS PharmSciTech*, **12**, 1366 (2011), <https://doi.org/10.1208/s12249-011-9705-z>
- <sup>35</sup> S. Elanthikkal, U. Gopalakrishnapanicker, S. Varghese and J. T. Guthrie, *Carbohydr. Polym.*, **80**, 852 (2010), <https://doi.org/10.1016/j.carbpol.2009.12.043>
- <sup>36</sup> N. Rehman, M. I. G. de Miranda, S. M. L. Rosa, D. M. Pimentel, S. M. B. Nachtigall *et al.*, *J. Polym. Environ.*, **22**, 252 (2014), <https://doi.org/10.1007/s10924-013-0624-9>
- <sup>37</sup> L. K. Kian, M. Jawaid, H. Ariffin and O. Y. Alothman, *Int. J. Biol. Macromol.*, **103**, 931 (2017), <https://doi.org/10.1016/j.ijbiomac.2017.05.135>
- <sup>38</sup> J. V. T. Lacaran, R. J. Narceda, J. A. V. Bilo and J. K. Leano Jr., *Cellulose Chem. Technol.*, **55**, 403 (2021), <https://doi.org/10.35812/CelluloseChemTechnol.2021.55.38>
- <sup>39</sup> A. G. Alhamzani and M. A. Habib, *Cellulose Chem. Technol.*, **55**, 33 (2021), <https://doi.org/10.35812/CelluloseChemTechnol.2021.55.04>
- <sup>40</sup> J. P. de Oliveira, G. P. Bruni, S. L. M. el Halal, F. C. Bertoldi, A. R. G. Dias *et al.*, *Int. J. Biol. Macromol.*, **124**, 175 (2019), <https://doi.org/10.1016/j.ijbiomac.2018.11.205>
- <sup>41</sup> M. Kazharska, Y. Ding, M. Arif, F. Jiang, Y. Cong *et al.*, *Int. J. Biol. Macromol.*, **134**, 390 (2019), <https://doi.org/10.1016/j.ijbiomac.2019.05.058>
- <sup>42</sup> J. P. S. Morais, M. D. F. Rosa, M. D. S. M. de Souza Filho, L. D. Nascimento, D. M. do Nascimento *et al.*, *Carbohydr. Polym.*, **91**, 229 (2013), <https://doi.org/10.1016/j.carbpol.2012.08.010>
- <sup>43</sup> A. Mandal and D. Chakrabarty, *Carbohydr. Polym.*, **86**, 1291 (2011), <https://doi.org/10.1016/j.carbpol.2011.06.030>
- <sup>44</sup> M. Thakur, A. Sharma, V. Ahlawat, M. Bhattacharya and S. Goswami, *Mater. Sci. Energ. Technol.*, **3**, 328 (2020), <https://doi.org/10.1016/j.mset.2019.12.005>
- <sup>45</sup> S. J. Byard, S. L. Jackson, A. Smail, M. Bauer and D. C. Apperley, *J. Pharm. Sci.*, **94**, 1321 (2005), <https://doi.org/10.1002/jps.20328>
- <sup>46</sup> A. Santmarti and K. Y. Lee, in “Nanocellulose and Sustainability”, edited by K. Y. Lee, CRC Press, 2018, pp. 67-86